Available online at www.sciencedirect.com
ScienceDirect
Trans. Nonferrous Met. Soc. China 23(2013) 1563−1569
Transactions of Nonferrous Metals Society of China
www.tnmsc.cn

Enhanced grain refinement of cast aluminum alloy by thermal and mechanical treatment of Al−5Ti−B master alloy

H. GHADIMI, S. HOSSEIN NEDJHAD, B. EGHBALI

Faculty of Materials Engineering, Sahand University of Technology, 51335-1996, Tabriz, Iran

Received 2 July 2012; accepted 13 November 2012

Abstract: Al_3Ti and TiB_2 particles with various sizes in Al−5Ti−B (mass fraction, %) master alloy were produced by liquid-phase isothermal annealing and plastic deformation. The results show that with decreasing the size of particles in the master alloy, the grain refining performance is improved but, the refinement of the particles is useful, and immoderate refining probably accelerates fading of particles, agglomeration, hence decreasing the grain refin efficiency.
Key words: Al−5Ti−B alloy; grain refinement; casting; inoculation; nucleation

1 Introduction

It is well known that an equiaxed grain structure manifests more enhanced mechanical isotropy than the columnar counterpart in solidification structure of cast metals. In addition, fine equiaxed grain structures exhibit improved casting properties such as surface quality, improved feeding to eliminate the shrinkage porosities, decreased hot tearing, and reduced mold filling time. For a long time, grain refining of cast structures has been practically employed by adding inoculants to the melt in foundry processes [1−5].

One of the most important grain refiners in aluminum casting is the Al−Ti−B master alloy, holding Ti/B ratios (mole ratio) of 3 and 5 [6−13]. Systematic studies on the effect of Ti/B ratio on the grain refining response of aluminum casting are indicative of the fact that the Al−5Ti−B master alloy is the more efficient grain refiner among all the compositions investigated [14]. Generally, two distinct approaches have been assumed for the mechanism of the nucleation: 1) particles paradigm, and 2) solute paradigm. The former suggests that the nucleation occurs on the borides (TiB_2 or others) and Al_3Ti particles present in the master alloy [1−3,7,8], while the latter assumes that both the existence of nucleant particles and the amount of segregating elements play an essential role in the grain refining process [2,7,15]. This segregating power of elements is quantified by the growth restricting factor (GRF) [16]. Consequently, it is assumed that Al_3Ti and TiB_2 particles present in the Al−5Ti−B master alloy provide heterogeneous nucleation sites for the solid grain [1−3,7, 8,15,17]. However, the size and morphology of those particles should be effective in the grain refinement. Following the fact, recent investigations have indicated that the fragmentation of Al_3Ti particles by means of plastic deformation such as rolling and extrusion improves the grain refining efficiency of Al−5Ti and Al−5Ti−B master alloys [14,18].

The aim of the present paper is to study the possibility of enhanced grain refinement of an aluminum cast metal by making the use of fragmented Al_3Ti and TiB_2 particles in an Al−5Ti−B master alloy. Various sizes of particles were provided by heat treatments and plastic deformation on a commercially-available Al−5Ti−B wire.

2 Experimental

A commercially-available Al−5Ti−B grain refiner wire with a diameter of 10 mm was used as the starting inoculation material. The starting master alloy was annealed at 900 °C for 24 h in order to stimulate the coarsened intermetallic particles. Furthermore, Al−5Ti−B master alloy was cold-rolled in order to fragment the existing intermetallic particles to reduce the size and increase the heterogeneous nucleating sites. A sample with a length of 250 mm and a diameter of 10 mm was cold-rolled to a thickness of 0.8 mm in several passes.

Corresponding author: H. GHADIMI; Tel: +98-412-3459449; Fax: +98-412-3444333; E-mail: Ghadimi629@gmail.com
DOI: 10.1016/S1003-6326(13)62631-X

Moreover, Al−5Ti−B master alloy was subjected to high pressure torsion (HPT) to accumulate severe plastic deformation for tremendous fragmentation of particles. The HPT was carried out for 5 turns of revolution under a pressure of 6 GPa. The starting Al−5Ti−B master alloy was also ball-milled into a very fine powder and, ultimately, two kinds of powders were produced: 1) small chips were cut from the starting master alloy and then ball-milled for 7, 30 and 50 h, respectively; 2) the chips prepared from the lower side of the annealed sample were ball-milled for 7 h. The ratio of ball to powder standing at 15:1 and the rotational speed of 400 r/min were used. These grain refiners were added to an aluminum melt at 800 °C via immersion, mechanical plunging and argon injection. The melt was poured into a cylindrical steel mould with an average diameter of 20 mm and a length of 70 mm. X-ray diffraction (XRD), optical microscopy (OM) and scanning electron microscopy (SEM) were used for structural examinations. The macrostructures of cast metals and the microstructure of Al−5Ti−B master alloy were revealed by etching in a standard Poulton's reagent and a 0.5% HF solution, respectively.

3 Results and discussion

Figure 1 shows the microstructures of the starting Al−5Ti−B master alloy with representing particle size from 0.1 to 40 μm. XRD pattern of this sample is shown in Fig. 2, which indicates the presence of Al_3Ti with a tetragonal crystal symmetry, TiB_2 with a hexagonal crystal symmetry (HCP) and α(Al) with a face-centered cubic (FCC) crystal symmetry. Occasionally, the classification of intermetallic particles was carried out on the basis of particle size. For example, TiB_2 particles are assumed to be in the diameter of 0.1−10 μm, while Al_3Ti particles are assumed to be in the diameter of 20−50 μm [13]. Meanwhile, VENKATESWARLU et al [18] showed that aforementioned size range is reduced for Al_3Ti particles after the extrusion. Figure 3 shows the microstructure of the Al−5Ti−B master alloy annealed at 900 °C for 24 h. This heat treatment corresponds to the liquid-solid two-phase region and shows that the Al_3Ti and TiB_2 particles are separated in accordance with the gravity segregation effect. In the upper region of the sample, large acicular particles are flocked; while in the lower region, the aggregation of smaller blocky particles occurs. SEM micrographs of the two sections are shown in Figs. 4 and 5. Two sections are divided precisely in order to clarify the structure and grain refining behavior

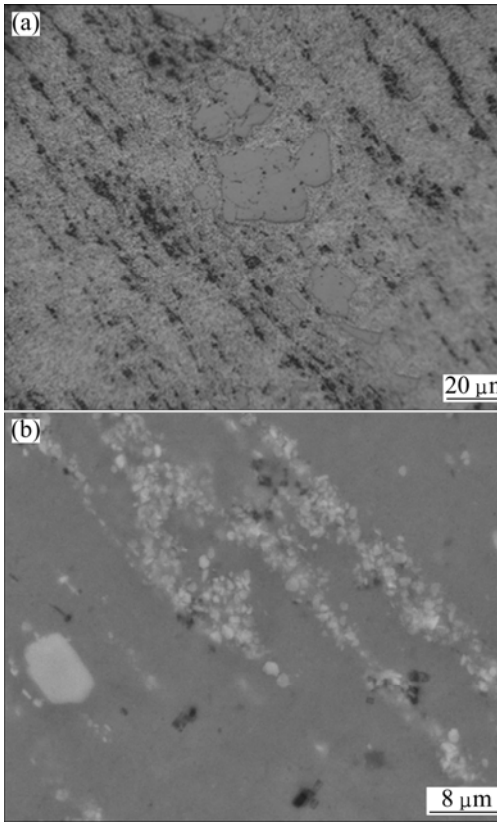

Fig. 1 Microstructures of as-received Al−5Ti−B master alloy: (a) OM; (b) SEM

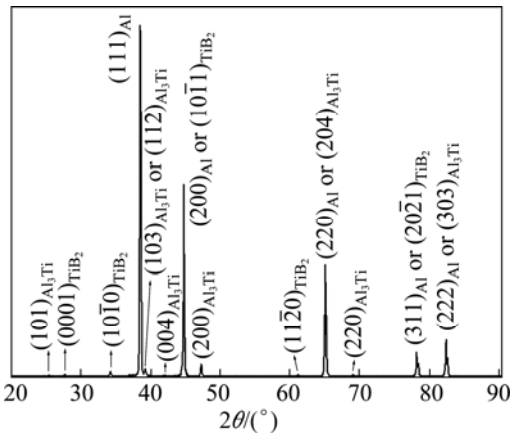

Fig. 2 XRD pattern of as-received Al−5Ti−B master alloy consisting of Al_3Ti, TiB_2 and Al

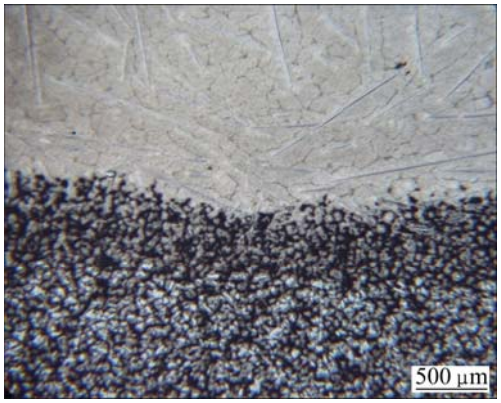

Fig. 3 Microstructure of annealed Al−5Ti−B master alloy showing gravity segregation of intermetallic particles

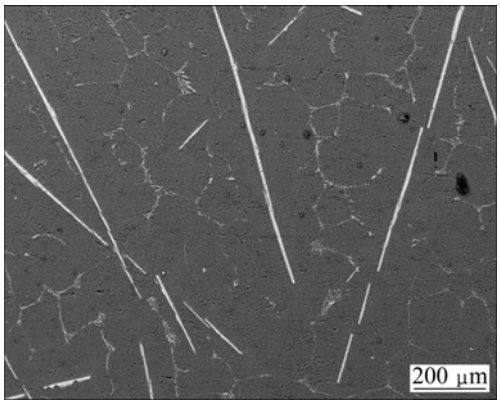

Fig. 4 SEM micrograph showing microstructural features of upper region of annealed sample including acicular particles

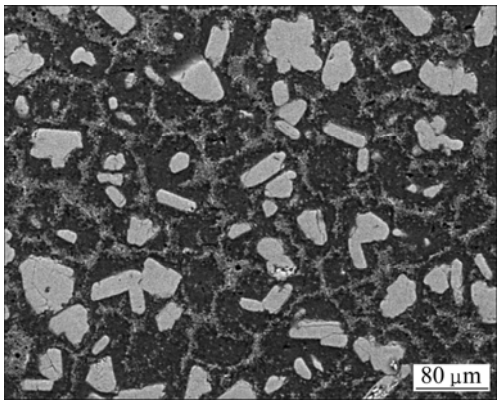

Fig. 5 SEM micrograph showing microstructural features of lower region of annealed sample including blocky particles

of the acicular and blocky particles separately. Figure 6 shows the XRD patterns of the annealed sample and those separated sections with starting sample. XRD analysis of the master alloys after heat treatment reveals an increase in the relative peak intensities of Al_3Ti and TiB_2, which could be related to solid-state precipitation of Al_3Ti from the supersaturated solid solution of Ti in Al [18] and coarsening of Al_3Ti and TiB_2 particles. Al_3Ti particles are coarsened more seriously than TiB_2 particles apparently.

Additionally, Fig. 6 shows that the upper section consists of Al_3Ti peaks. This is reasonable since the density of Al_3Ti particles is 3.35 g/cm^3, which is smaller than that of TiB_2 (4.52 g/cm^3). Accordingly, it is rationalized that the Al_3Ti and TiB_2 particles get segregated into the upper and lower regions during the annealing process, respectively, although the large white-gray blocky particles in the lower region could be Al_3Ti simultaneously. What follows, Fig. 7 shows the SEM micrograph from the lower section, indicating a bimodal particle-size distribution consisting of coarse and fine particles.

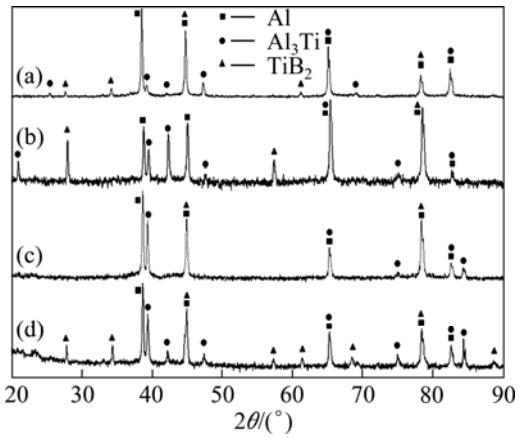

Fig. 6 XRD patterns of Al−5Ti−B master alloy: (a) Starting material as reference; (b) Annealed specimen; (c) Upper part of annealed specimen; (d) Lower part of annealed specimen

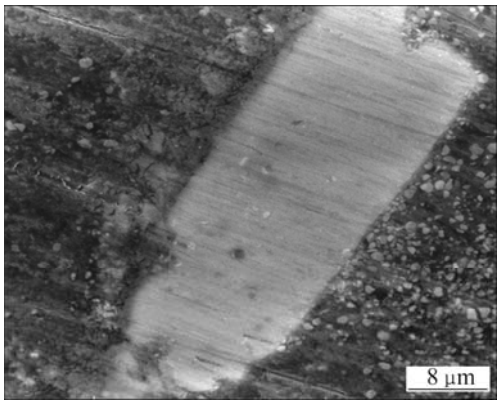

Fig. 7 SEM micrograph from lower section of annealed alloy showing bimodal particle size distribution

Figure 8 shows the fragmentation of Al_3Ti particles during cold rolling. This operation leads obviously to a decrease in the size and increase in the number of particles. To operationalize another trend of work, Fig. 9 shows the microstructure of Al−5Ti−B after HPT operation in which a uniform dispersion of particles is observed in Al matrix.

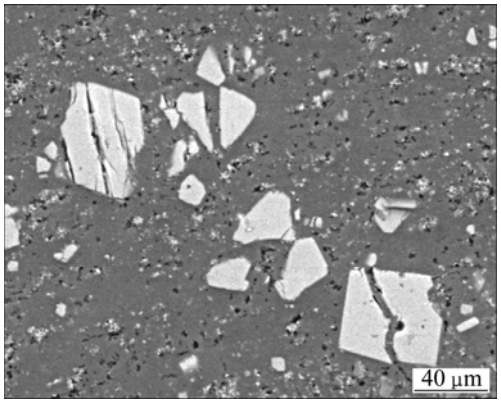

Fig. 8 Fragmentation of particles in Al−5Ti−B master alloys by cold rolling

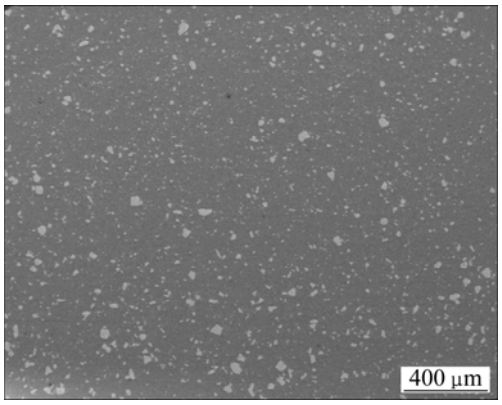

Fig. 9 Microstructure of Al−5Ti−B after HPT showing uniform dispersion of particles

Figure 10 shows the XRD patterns of the powder samples ball-milled for various times. Notably, the relative intensity of Al_3Ti drastically decreases in a specimen ball-milled for 50 h and an existence of Al_2O_3 diffraction line at intermediate milling time is denoted. Figure 11 shows the XRD patterns of ball-milled chips belonging to the lower part of the annealed sample that consists of blocky particles.

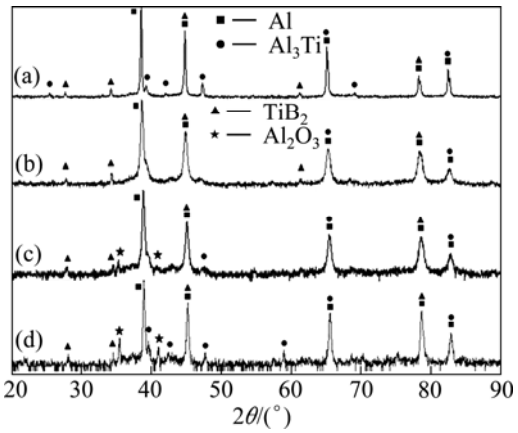

Fig. 10 XRD patterns of Al−5Ti−B master alloy ball-milled for different times: (a) Starting material; (b) Ball-milled for 50 h; (c) Ball-milled for 30 h; (d) Ball-milled for 7 h

The photomacrographs of cast aluminum metals are shown in Fig. 12, showing that grain refining is effective when the mass fraction of Al−5Ti−B master alloy exceeds 0.2% and is saturated at about 1%. Figure 13 shows the macrostructures of cast aluminum metals inoculated with the processed Al−5Ti−B master alloys with different mass fractions. In comparison with the as-received metal, the rolled master alloy shows the enhanced grain refinement, in which the minimum grain size corresponds to the mass fraction of Al−5Ti−B master alloy of 3%.

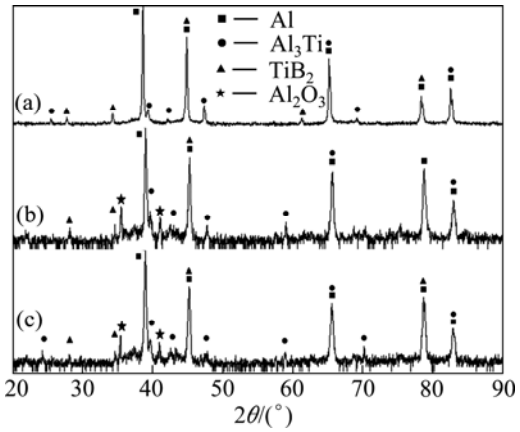

Fig. 11 XRD patterns of Al−5Ti−B master alloy: (a) Starting material; (b) Starting material ball-milled for 7 h; (c) Chips from lower part of annealed sample ball-milled for 7 h

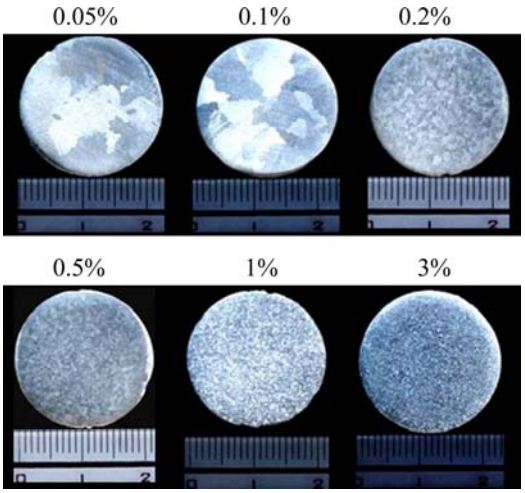

Fig. 12 Macrostructures of cast aluminum metals inoculated with as-received Al−5Ti−B master alloy with various mass fractions

Inoculants separated from the upper side of the annealed sample in Fig. 13(c) show weak grain refinement. The coarsening of Al_3Ti particles and the absence of TiB_2 particles can be two reasons for this decline. However, the samples separated from the lower side of the annealed master alloy, including blocky particles, show the enhanced grain refinement, even better than the cold-rolled metal. A mixture of the lower and upper side of the annealed metal shows weak grain refinement as demonstrated in Fig. 13(e). These observations confirm that the growth restricting factor (GRF) could not explain the mechanism of the grain refinement. The morphology, size and type of particles are important too. The nucleation potential of TiB_2 particles is better than that of Al_3Ti particles, but the presence of Al_3Ti particles improves the grain refinement efficiency. It can be contributed to increasing the

nucleation sites, preventing the dissolution of boron in the melt and the very high segregating power of Ti. Ti segregates to the nucleant–liquid interface, which leads to constitutional supercooling, and other nucleant particles get activated for the nucleation. Unexpectedly, a sample deformed by HPT shows weak grain refinement, as indicated in Fig. 13(f), which can be contributed to the agglomeration and fading effects of the fragmented particulates. The macrostructures of aluminum casting inoculated with ball-milled powders are shown in Fig. 14. It is found that the powder injected by argon stream is hardly effective, while mechanical injection is effective.

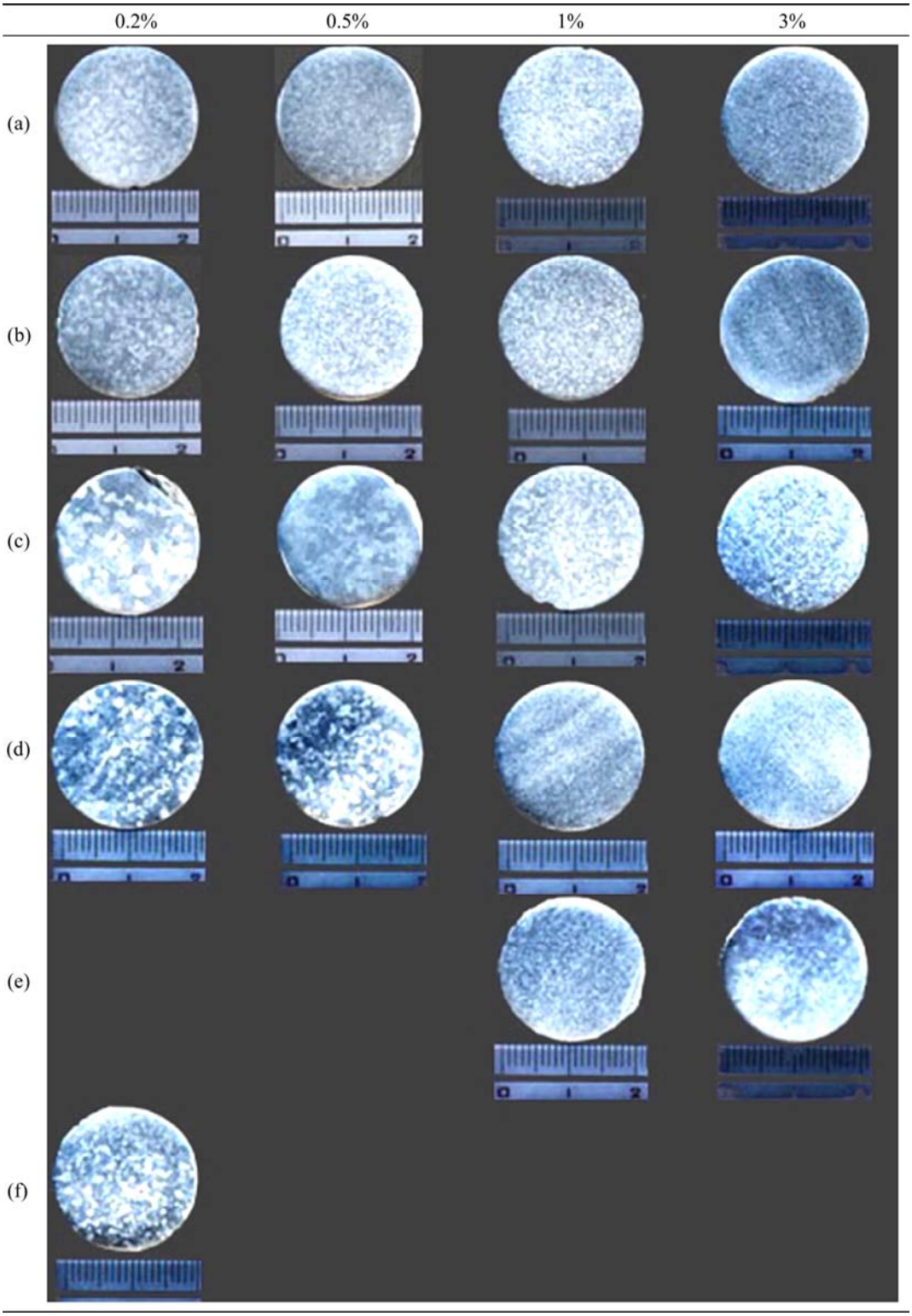

Fig. 13 Macrostructures of cast aluminum metals inoculated with Al−5Ti−B master alloy with various mass fractions: (a) Starting material as reference; (b) Rolled specimen; (c) Upper part of annealed specimen; (d) Lower part of annealed specimen; (e) Annealed specimen; (f) HPT

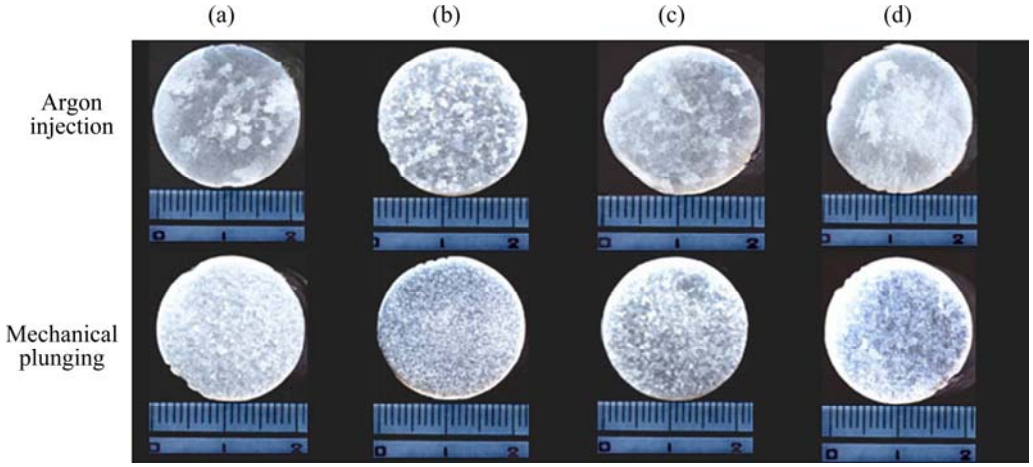

Fig. 14 Macrostructures of cast aluminum metals inoculated with Al−5Ti−B master alloy at mass fraction of 0.5%: (a) Starting material ball-milled for 7 h; (b) Chips from lower part of annealed sample ball-milled for 7 h; (c) Starting material ball-milled for 30 h; (d) Starting material ball-milled for 50 h

4 Conclusions

1) Cold rolling of the Al−5Ti−1B master alloy improves its grain refining efficiency. Rolling induces the fragmentation of particles, thus increasing the number of effective nucleating sites for Al.

2) Annealing of Al−5Ti−B mater alloy stimulates the intermetallic particle gravity segregation. The lower part of the annealed sample shows the most grain refinement potency.

3) The growth restriction effect in the grain refinement is important, but the type and size of particles play a vital role in the grain refinement.

4) By decreasing the size of the particles, the grain refining performance is improved but, refining of the particles is useful somewhat, and immoderate refining probably accelerates fading of particles, agglomeration hence decreasing of the grain refining efficiency.

5) Mechanical plunging of ball-milled powders shows the enhanced grain refinement.

References

[1] MURTY B S, KORI S A, CHAKRABORTY M. Grain refinement of aluminium and its alloys by heterogeneous nucleation and alloying [J]. International Materials Reviews, 2002, 47(1): 3−29.

[2] EASTON M, STJOHN D. Grain refinement of aluminum alloys: Part I. The nucleant and solute paradigms—A review of the literature [J]. Metallurgical and Materials Transactions A, 1999, 30(6): 1613−1623.

[3] KASHYAP K T, CHANDRASHEKAR T. Effect and mechanism of grain refinement in aluminum alloys [J]. Bulletin of Material Science, 2001, 24(4): 345−353.

[4] ZHU Man, YANG Gen-cang, YAO Li-juan, CHENG Su-ling, ZHOU Yao-he. Influence of Al−Ti−B addition on the microstructure and mechanical properties of A356 alloys [J]. Rare Metals, 2009, 28(2): 181−186.

[5] BENNY KARUNAKAR D, RAM NARESH R, SUPRAKASH P, DATTA G L. Effects of grain refinement and residual elements on hot tearing in aluminum castings [J]. The International Journal of Advanced Manufacturing Technology, 2009, 45(9−10): 851−858.

[6] CIBULA A. The grain refinement of aluminium alloy castings by additions of titanium and boron [J]. Journal of the Institute of Metals, 1951−1952, 80: 1−16.

[7] QUESTED T E. Understanding mechanism of grain refinement of aluminium alloys by inoculation [J]. Journal of Materials Science, 2004, 20(11): 1357−1369.

[8] MOHANTY P S, GRUZLESKI J E. Mechanism of grain refinement in aluminium [J]. Acta Materialia, 1995, 43(5): 2001−2012.

[9] JONES G P, PEARSON J. Factors affecting the grain refinement of aluminum using titanium and boron additives [J]. Metallurgical Transactions B, 1976, 7(2): 223−234.

[10] MOLDOVAN P, POPESCU G. The grain refinement of 6063 aluminum using Al−5Ti−1B and Al−3Ti−0.15C grain refiners [J]. JOM, 2004, 56(11): 59−61.

[11] YU L, LIU X, WANG Z, BIAN X. Grain refinement of A356 alloy by AlTiC/AlTiB master alloys [J]. Materials Science, 2005, 40(14): 3865−3867.

[12] DAVIES I G, DENNIS J M, HELLAWELL A. The nucleation of aluminum grains in alloys of aluminum with titanium and boron [J]. Metallurgical Transactions, 1970, 1(1): 275−280.

[13] GREER A L, BUNN A M, TRONCHE A, EVANS P V, BRISTOW D J. Modelling of inoculation of metallic melts: Application to grain refinement of aluminium by Al−Ti−B [J]. Acta Materialia, 2000, 48(11): 2823−2835.

[14] VENKATESWARLU K, MURTY B S, CHAKRABORTY M. Effect of hot rolling and heat treatment of Al−5Ti−1B master alloy on the grain refining efficacy of aluminium [J]. Materials Science and Engineering A, 2001, 301(2): 180−186.

[15] EASTON M, STJOHN D. Grain refinement of aluminum alloys: Part II. Confirmation of, and a mechanism for, the solute paradigm [J]. Metallurgical and Materials Transactions A, 1999, 30(6): 1625−1633.

[16] CHANDRASHEKAR T, MURALIDHARA M K, KASHYAP K T, RAGHOTHAMA RAO P. Effect of growth restricting factor on grain refinement of aluminum alloys [J]. The International Journal of

Advanced Manufacturing Technology, 2009, 40(3−4): 234−241.

[17] SCHUMACHER P, GREER A L, WORTH J, EVANS P V, KEARNS M A, FISHER P, GREEN A H. New studies of nucleation mechanisms in aluminium alloys: Implications for grain refinement practice [J]. Materials Science and Technology, 1998, 14(11): 394−404.

[18] VENKATESWARLU K, DAS S K, CHAKRABORTY M, MURTY B S. Influence of thermo-mechanical treatment of Al−5Ti master alloy on its grain refining performance on aluminium [J]. Materials Science and Engineering A, 2003, 351(1−2): 237−243.

Al−5Ti−B 中间合金的热机械处理对铸造铝合金晶粒细化的强化作用

H. GHADIMI, S. HOSSEIN NEDJHAD, B. EGHBALI

Faculty of Materials Engineering, Sahand University of Technology, 51335-1996, Tabriz, Iran

摘　要：采用等温液相退火和塑性变形工艺制备含不同尺寸 Al_3Ti 和 TiB_2 粒子的 Al−5Ti−B(质量分数，%)中间合金。结果表明：随着中间合金中 Al_3Ti 和 TiB_2 粒子尺寸的减小，合金的晶粒细化作用得到增强，但不适当地减小 Al_3Ti 和 TiB_2 的粒径可能导致这些颗粒作用减弱和结块，从而降低合金的晶粒细化效率。

关键词： Al−Ti−B 合金；晶粒细化；铸造；自孕育；形核

(Edited by Wei-ping CHEN)